Talanta 115 (2013) 830–836

Contents lists available at SciVerse ScienceDirect

Talanta

journal homepage: www.elsevier.com/locate/talanta

Highly sensitive resonance light scattering bioassay for heparin based on polyethyleneimine-capped Ag nanoclusters

Yurong Tang [a], Yu Zhang [a], Yingying Su [b], Yi Lv [a,*]

[a] Key Laboratory of Green Chemistry & Technology, Ministry of Education, College of Chemistry, Sichuan University, Chengdu 610064, China
[b] Analytical & Testing Center, Sichuan University, Chengdu, Sichuan 610064, China

ARTICLE INFO

Article history:
Received 8 April 2013
Received in revised form
8 June 2013
Accepted 16 June 2013
Available online 5 July 2013

Keywords:
PEI-capped Ag NCs
In-situ reduction
Resonance light scattering
Heparin

ABSTRACT

Ag nanoclusters (NCs) possessed distinct physical and chemical attributes that made them excellent scaffolds for the development of novel bio-analytical methodology. In the present work, a green approach for the preparation of Ag nanoclusters (NCs) was proposed on the basis of templated polyethyleneimine (PEI) assisted in-situ reductive crystallization of Ag (I), and then a sensitive resonance light scattering bioassay for the determination of heparin was established on the basis of the enhanced resonance light scattering of the PEI-capped Ag NCs during the presence of heparin. Further investigation indicated that the molecular weight of PEI, the PEI/Ag (I) ratio and the pH value of reaction conditions had great influence on the formation of Ag NCs, which was directly correlated to resonance light scattering. The bioassay allows sensitive and selective detection of heparin with a detection limit of 27.5 nM, and successfully applied for the determination of heparin in human serum samples.

1. Introduction

Metal nanoclusters, which consist of only several to tens of metal atoms and possess sizes comparable to the Fermi wavelength of electrons, have drawn considerable attentions owning to their unique properties in the areas of catalysts, optoelectronic devices, bioassays, biolabelling, clean energy sources, chemical and biological sensors and environmental analysis [1–8]. Among various metallic NCs, Au and Ag NCs are the most popular because of their intrinsic characteristics such as large Stokes shift, tunable emission colors, water solubility and biocompatibility [9–13]. In the past decades, Au NCs with their ease of preparation and chemical stability have been extensively studied [14–19]. Comparatively, fewer studies have focused on preparing Ag NCs, because these clusters are often instable in water and have a natural tendency to aggregate to form larger non-fluorescent plasmonic silver nanoparticles by most synthetic procedure [20].

To avoid this aggregation, templates or capping agents such as DNA [21], protein [22,23], peptide [24], thiolates [25,26], dendrimers [27], polymer microgels [28,29] and polyelectrolyte [30] are required for synthesis of Ag nanoclusters in aqueous solutions. However, environmentally harmful UV irradiation/γ-irradiation or toxic sodium borohydride were always employed as the reducing medium in the above-mentioned cases. Recently, polyethyleneimine was also demonstrated as an ideal template to generate highly fluorescent Ag NCs [31]. Nevertheless, this synthesis required excess amounts of formaldehyde as reducing agents, which are not only environmentally harmful but also unavoidably apt to form large Ag nanoparticles. Since PEI itself could serve as a promising reducing agent in the preparation of Au or Ag nanoparticles [32,33], we postulated that a green approach for the preparation of Ag nanoclusters might be realized by rational controlling the reducing property of PEI via judicious selecting the structure of PEI and optimizing the reaction conditions. Herein, we reported a simple, one-pot, “green” synthetic route for the preparation of fluorescent PEI-caped Ag NCs at room temperature under pH 9. Microwave, which has been known as an efficient and green style with reduced reaction time [34,35], was adopted in the present study.

On the other hands, heparin, a highly sulfated polysaccharide with an average charge up to ~70, is used in different forms in anticoagulation treatment [36]. Thus, monitoring the amount of heparin used during the surgery and the anticoagulant therapy is of crucial significance. Up to now, there have been several approaches for the determination of heparin [37–39]. Nevertheless, a sensitive, reliable and easily operated detection method for heparin is still expected. Few works, so far, have been reported regarding the foundation of resonance light scattering (RLS)-based protocols to directly detect target molecules utilizing nanocrystals [6]. Our preliminary experiments indicated that the heparin could obviously enhance resonance light scattering of the prepared Ag NCs. Therefore, the objective of this study was to develop a facile resonance light scattering bioassay for sensitive and selective

* Corresponding author. Tel./fax: +86 28 8541 2798.
E-mail address: lvy@scu.edu.cn (Y. Lv).

0039-9140/$ - see front matter © 2013 Elsevier B.V. All rights reserved.
http://dx.doi.org/10.1016/j.talanta.2013.06.028

detection of heparin in biological fluids via a strategy of the target-involved assembly of the prepared PEI-capped Ag NCs.

2. Experimental

2.1. Chemicals and materials

Deionized water with conductivity of 18.2 MΩ cm^{-1} was used in this experiment from a water purification system (ULUPURE, Chengdu, China). $AgNO_3$ was from Shanghai chemical regent Co. Ltd. Heparin sodium purchased from Aladdin (Shanghai, China) has 185 USP units/mg. Polyethyleneimine (PEI, branched, MW600, 1800, and 10,000, 99%) was bought from Aladdin (Shanghai, China). HSA, GSH, Cys and calf thymus DNA were purchased from Solarbio Science & Technology Co. Ltd. (Beijing, China). Hyaluronic acid sodium (HA), Adenosine 5′-triphosphate (ATP), dextran and all amino acids were purchased from Aladdin (Shanghai, China), and all the other reagents were at least of analytical grade.

2.2. Apparatus and measurements

Transmission electron microscopy (TEM) and high-resolution transmission electron microscopy (HRTEM) of PEI-capped Ag NCs were carried out on a Tecnai G2 F20 S-TWIN transmission electron microscope at an accelerating voltage of 200 kV (FEI Co., America). Samples were prepared for analysis by evaporating a drop of aqueous product on a lacey carbon copper TEM grid. Dynamic light scattering (DLS) were performed with a Zetasizer Nano ZS (Malvern Co., UK). X-ray photoelectron spectroscopy (XPS) was performed with a XSAM 800 electron spectrometer (Kratos) using monochromatic Al Ka radiation for the analysis of the surface composition and chemical states of the product. Matrix-assisted laser desorption/ionization-time of flight mass (MALDI-TOF-MS) spectra were measured on an Ultraflex III TOF/TOF (Bruker Daltonics GmbH, Bremen, Germany). 2,5-Dihydroxybenzoic acid (DHB) was used as the matrix to enhance ionization. The UV–vis spectra and the photoluminescence spectra were obtained with a U-2910 UV–vis spectrophotometer and an F-7000 fluorescence spectrophotometer (Hitachi Co., Tokyo, Japan). The resonance light scattering (RLS) measurements were also performed on the spectrofluorometer. Fourier Transform Infrared spectra (FTIR) from 4000 to 400 cm^{-1} was recorded in KBr discs on a Nicolet IS10 FTIR spectrometer (Thermo Inc., America) for evaluating the encapsulation of PEI and PEI-capped Ag NCs. XRD patterns of the samples were recorded using X′Pert Pro X-ray diffractometer (Philips) with Co Kα radiation ($\lambda = 1.79$ Å). The samples of silver nanoclusters were taken on a glass plate and the X-ray diffractogram was collected in the 2θ range of 20–95°.

2.3. Preparation of PEI-capped Ag NCs

In a typical synthesis, 0.5 ml of 0.1 M $AgNO_3$ and 0.3 mL of 0.425 g mL^{-1} PEI were added into 0.2 mL H_2O, the pH value of which was adjusted to 9.0 by HNO_3 (1 M) and homogenized by stirring. Then the mixture solution was treated in a domestic microwave oven for 2 min and was subsequently centrifuged at 12,000 rpm for 10 min to remove byproducts of large particles. The light-yellow supernatant containing the Ag NCs was collected. A dialysis membrane was then used to separate the Ag NCs from

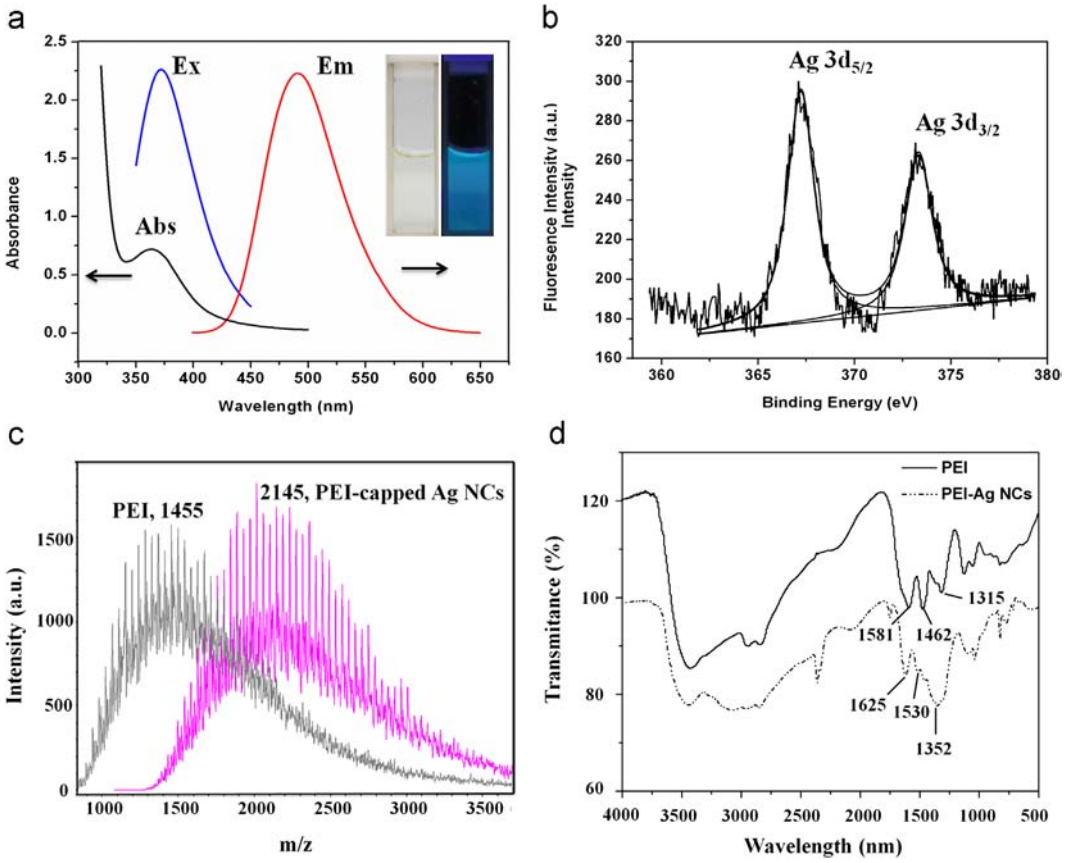

Fig. 1. (a) The optical properties of the Ag NCs: the UV–vis absorption (curve black) and the fluorescence excitation (curve blue) and emission (curve red); inset of (a) shows photographs of the solution of Ag NCs under ambient light (left) and UV light (right); (b) XPS spectra of the Ag NCs; (c) MALDI-TOF-MS spectra of PEI (gray) and PEI-capped Ag NCs (pink); and (d) FTIR spectra of the PEI-capped Ag NCs and PEI. (For interpretation of the references to color in this figure legend, the reader is referred to the web version of this article.)

all residual unreacted species. The as-prepared purified Ag NCs solution was stored at 4 °C in the dark for further use. The concentration of the as-prepared Ag NCs solution was defined as it contained silver concentration which was determined by ICP-MS. Furthermore, in order to optimize the synthetic condition for specific particle sizes and associated property variations, extensive experiments were also carried out by varying the PEI molecular weight, pH and $AgNO_3$/PEI weight ratio.

2.4. Detection of heparin

One hundred μL of the as-prepared Ag NCs, 400 μL of heparin standard solution or ultrafiltrated serum sample and a suitable volume of water were mixed to get 2 mL of solution. The resultant mixture was gently stirred for 20 min, and then the RLS signal was monitored. The RLS measurements were carried out in the absence or presence of heparin when the spectrofluorometer was set in the synchronous mode with the slit width of 5 and 5 nm for excitation and emission. The photomultiplier tube (PMT) voltage was set at −400 V.

The human serum samples were obtained from Chengdu 7th People's Hospital, China. The serum samples are filtrated with Amicon Ultra-4 centrifugal Filter Units (30 kDa) by centrifugation at 6000 rpm for 15 min before detection.

3. Results and discussion

3.1. Characterization of PEI-capped Ag NCs

In this study, Ag NCs, soluble in water, were prepared by a facile one-phase process. In a typical synthesis, a freshly prepared mixture solution of $AgNO_3$ and PEI 1800 was adjusted to pH 9 by HNO_3, and then irradiated by microwave for 2 min (Fig. S1). The resultant products were obtained by centrifugation and dialysis. The as-prepared Ag nanoclusters exhibited strong fluorescence emission at 492 nm with the excitation at 372 nm (Fig. 1a). The quantum yield of the PEI-capped Ag NCs was calculated to be about 12% with quinine sulfate as the reference. Its XPS spectra with two peaks at about 368.7, and 373.2 eV demonstrated the presence of Ag^0 (Fig. 1b). The formation of small clusters in the reaction was further confirmed by the X-ray diffraction pattern (Fig. S2), which showed a broad peak, and no characteristic peaks were observed for silver clusters formed in the synthesis [25]. MALDI-TOF-MS spectra showed the PEI molecular weight to be ~1500, the as-prepared Ag NCs showed a peak shift of 690 (Fig. 1c), which could be attributed to the 6 silver atoms in the Ag NCs. From the FTIR spectra of PEI and PEI-capped Ag NCs (Fig. 1d), the peaks of amino-groups at 1581, 1462, and 1315 cm^{-1} shifted to 1625, 1530, and 1352 cm^{-1} which could be attributed to the formation of imine, after PEI reacted with $AgNO_3$. These changes indicated that the protonated amine and neighboring methylene dehydrogenate to form a labile double bond (C=N) intermediate, which transforms into imine [40].

3.2. Molecular weight of PEI dependent on the synthesis of Ag NCs

The effect of PEI structure on the synthesis of Ag NCs was examined. We found that the molecular weight of PEI had a great influence on the preparation of Ag NCs. Accordingly, when using PEI of different molecular weights, such as 600, 1800, and 10,000 g/mol, to synthesize Ag NCs, the average size of the corresponding resultant particle increased with increasing PEI molecular weight (Fig. 2). The resultant PEI-600 and PEI-1800 capped Ag NCs displayed strong fluorescence with the absorption peak at 362 nm (Fig. 2a and b) and the average hydrodynamic

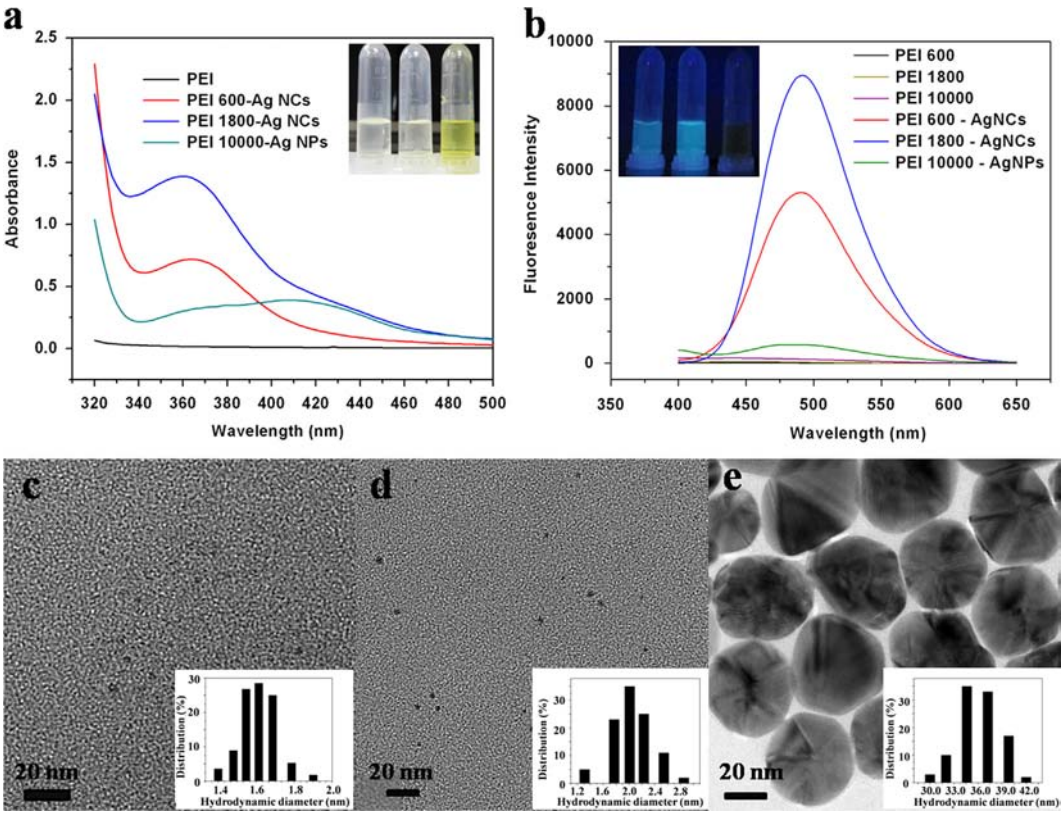

Fig. 2. (a) UV–vis spectra and (b) fluorescence emission spectra of the Ag NCs capped with PEI of different molecular weight. Photographs of these Ag NCs under ambient light (inset of (a)) and UV light (inset of (b)). TEM images of PEI 600-capped Ag NCs (c); PEI 1800-capped Ag NCs (d); and PEI 10000-capped Ag NPs (e). Scale bar: 20 nm. Inset of (c) and (d) shows the DLS histogram of these Ag NCs and Ag NPs.

diameter was calculated as 1.6 ± 0.1 and 2.0 ± 0.2 nm, respectively (Fig. 2c and d). However, PEI-10000 only led to the formation of larger non-fluorescent nanoparticles and displayed apparent surface plasmon resonance absorption peak in the range of 400–500 nm (Fig. 2a), the average hydrodynamic diameter was calculated as 34.6 ± 3.5 nm (Fig. 2e). It was postulated that the correlation between the crystal size and the molecular weight of PEI possibly resulted from an increasing amount of Ag (I) associated within larger polymer chains [41,42].

3.3. PEI/Ag(I) ratio dependent on the synthesis of Ag NCs

Apart from the molecular weight of PEI, the ratio of the reagents also affected the preparation of Ag NCs (Figs. 3 and S3). As the PEI concentration decreased respective to Ag (I), the higher Ag (I) concentration in PEI chains led to the agglomeration and the formation of larger nanoparticles. This indicated that PEI was effective to bind the Ag NCs and prevented them from growing further at the high PEI/Ag ratio [43].

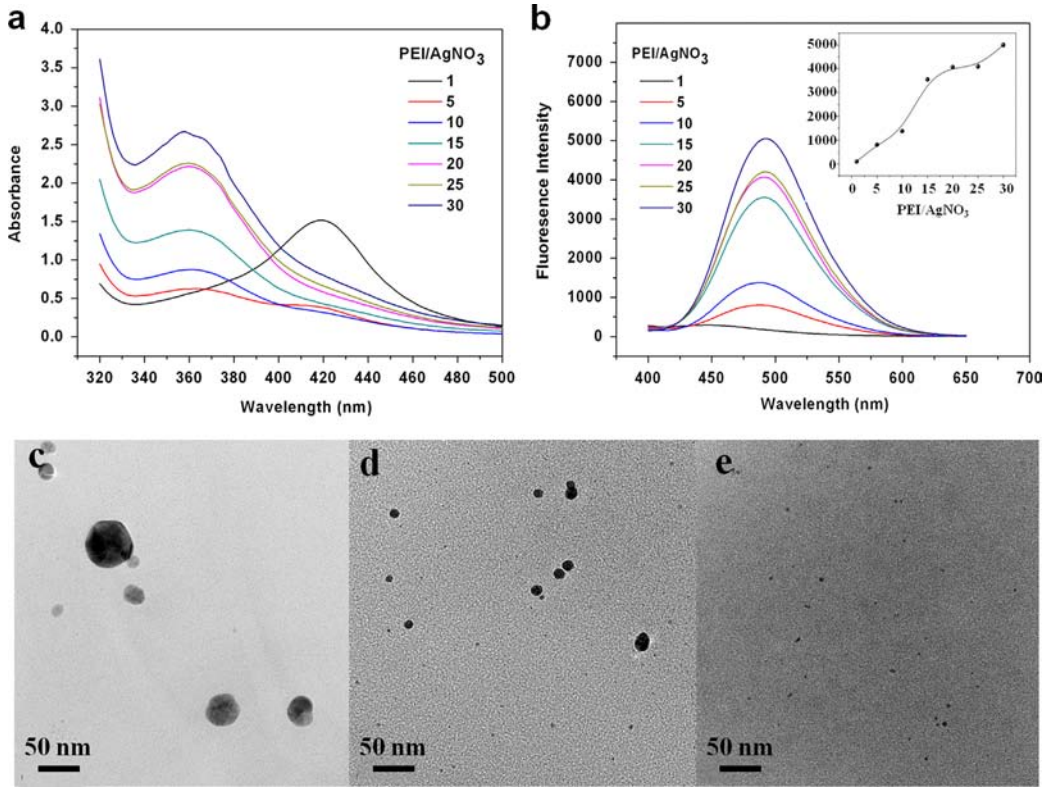

Fig. 3. (a) UV-Vis spectra and (b) Fluorescence emission spectra of PEI 1800-capped Ag NCs solutions synthesized at different $PEI/AgNO_3$ ratio. The inset of (b) showed the fluorescence intensity at 492 nm at different $PEI/AgNO_3$ ratio. TEM images of PEI-1800 capped Ag NCs synthesized at $PEI/AgNO_3$ ratio = 1 (c), $PEI/AgNO_3$ ratio = 5 (d) and $PEI/AgNO_3$ ratio = 20 (e). All the scale bars are 50 nm.

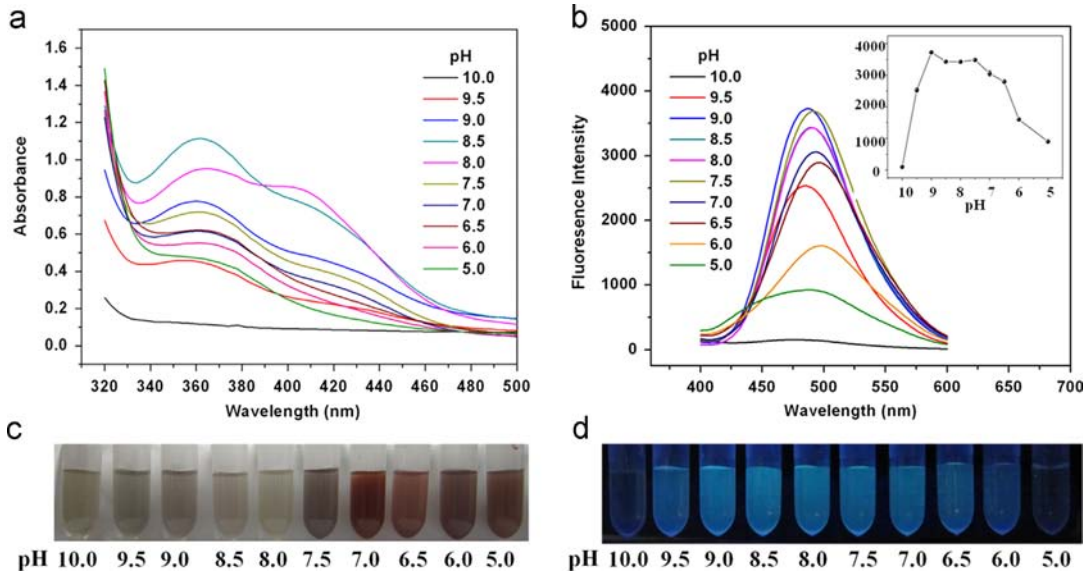

Fig. 4. pH-dependent of PEI 1800-capped Ag NCs synthesized. (a) UV–vis spectra and (b) fluorescence emission spectra of Ag NCs. The inset of (b) shows the fluorescence intensity at 492 nm at different pH value. Photographs of Ag NCs at different pH condition under ambient light (c) and UV light (d).

3.4. pH value dependent on the synthesis of Ag NCs

The effect of pH on the preparation of Ag NCs was also investigated (Figs. 4 and S4). As shown in the emission spectra (Fig. 4a) and UV–vis absorption spectra (Fig. 4b) of the PEI 1800-capped Ag NCs at pH 10.0 to 5.0, the maximum fluorescence intensity was observed in a pH range of 9.0–7.5, and the nanoclusters synthesized at either lower or higher pH value exhibited weaker fluorescence intensity. It was known that few amino groups of PEI (pK_a=9.64) were protonated at pH above 10.0, thus it might result in sluggish reduction of Ag(I) due to the strong interaction between Ag(I) and lone pairs of amino groups [44], and therefore only limited nanoclusters were produced. On the other hand, at lower pH, weak interaction between Ag(I) and PEI led to easy reduction of Ag(I) with the formation of huge amounts of Ag nanoparticles, which was in accord with the observed absorption bands at 410 nm (Fig. 4a) as well as the evidences from the color evolution (Fig. 4c) and the TEM images (Fig. S5). Therefore, the control of the pH was also crucial for the preparation of highly fluorescent Ag NCs.

3.5. RLS detection of heparin by PEI-capped Ag NCs

Since heparin is the highly negative charged linear polysaccharide and the Ag NCs capped with abundant amino groups of PEI are highly positive charged, the target-induced electrostatic self-assembly is consequently expected (Fig. 5). Initial FL detection of heparin by as-prepared PEI-capped Ag NCs was engaged, however, the detection limit was not promising. Pleasingly, we found that the resonance light scattering of the as-prepared Ag NCs was

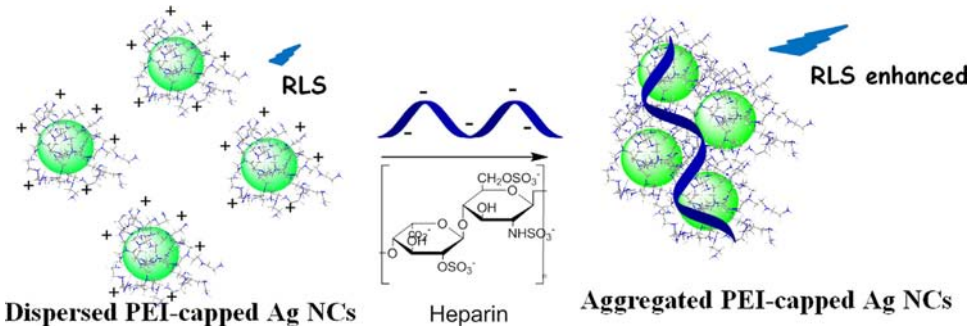

Fig. 5. The scheme for RLS detection of heparin via a strategy of the target induced self-assembly of PEI-capped Ag NCs.

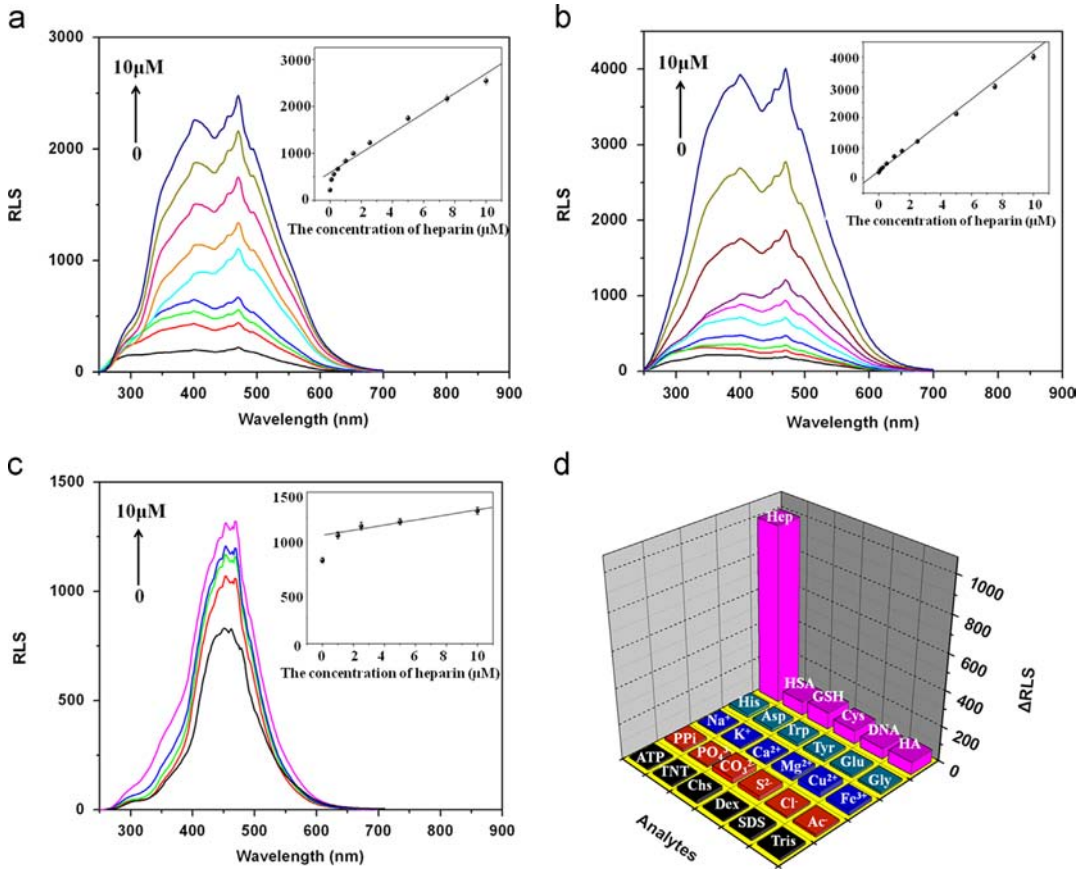

Fig. 6. RLS response of (a) PEI 600-capped Ag NCs; (b) PEI 1800-capped Ag NCs; (c) PEI 10000-capped Ag NPs (Ag NCs and Ag NPs concentration at 0.21 mM as Ag) to heparin. Inset of (a)–(c) showed linear plots of the RLS at 400 nm against the concentration of heparin. (d) RLS response of the PEI-capped Ag NCs in the presence of various analytes: heparin (1 μM), HSA (5 μg mL^{-1}), IgG (5 μg mL^{-1}), GSH (10 μM), Cys (10 μM), calf thymus DNA (50 ng mL^{-1}), amino acids (1 mM), Na^+, K^+, Ca^{2+}, Mg^{2+},Cu^{2+}, Fe^{3+} (10 mM), and PPi, PO_4^{3-},CO_3^{2-}, S^{2-},Cl^-, Ac^- (10 mM) and ATP, TNT, chitosan, dextran, SDS, Tris (1 mM).

readily enhanced in the presence of heparin. Upon adding heparin, the RLS signal of PEI-capped Ag NCs increased enormously and reached the maximum within 20 min and kept stable in the subsequent 60 min (Fig. S6a). It can be seen that the optimum pH was about 7 (Fig. S6b). If the acidity is higher or lower, the relative RLS intensities of the heparin reaction decreased.

We observed that the different particle size of PEI-capped Ag NCs and or Ag NPs could result in different binding tendency of heparin and thus leading to different sensitivity and detection windows. Calibration graphs of RLS intensities against concentration of heparin were constructed and are shown in Fig. 6a–c. The results were listed in Table 1. PEI 1800-capped Ag NCs was demonstrated to exhibit more excellent sensitivity (detection limit (DL) is 27.5 nM) and detection window (0.1–10 μM) than that of PEI 600-capped Ag NCs and PEI 10000-capped Ag NPs. Compared Ag NCs to Ag NPs, the amount of small particles in the solution was much more than that of the big ones and the small particles are also much easier to aggregate than big ones, which led to a higher sensitivity. Compared PEI 600-capped Ag NCs to PEI 1800-capped Ag NCs, the lower feed amount of PEI resulted in the lower loading amount of ligand and the lower loading amount of the positive amino groups on the surface of Ag NCs afforded the less binding sites to the negative analytes, which led to the narrower detection window [37]. Moreover the variation in concentration Ag NCs also affected the sensitivity and detection window of analytes, 0.21 mM of the as-prepared Ag NCs solution was selected as the optimal concentration in future research (Fig. 7). Higher concentration of the Ag NCs solution gave higher sensitivity, but narrower linear range [6,37].

A facile RLS method for sensitive and selective detection of heparin was thus demonstrated via a strategy of the target involved assembly of PEI-capped Ag NCs. TEM indicated good dispersibility of the PEI-capped Ag NCs with slight random agglomerations (Fig. S7). Upon adding 5 μM heparin, Ag NCs assembled to form larger clusters. The aggregation of the Ag NCs on the biological macromolecule would greatly enhance the intensity of RLS [45–48].

Table 1
Analytical figures of merit of RLS assay of heparin based on PEI-capped Ag NCs.

	Calibration function	Linear range (μM)	DL (nM)	Precision (RSD,%)
PEI 600-Ag NCs	$Y=211.0X+607.7$	0.8–10.0 ($R=0.9940$)	51.4	1.2
PEI 1800-Ag NCs	$Y=397.3X+232.1$	0.1–10.0 ($R=0.9926$)	27.5	1.7
PEI 10000-Ag NPs	$Y=25.2X+1073.2$	1.0–10.0 ($R=0.9733$)	245.6	2.3

3.6. Selectivity of RLS detection of heparin by PEI-capped Ag NCs

Study on the RLS response of the PEI-capped Ag NCs to various analytes showed good selectivity of the present assay for heparin. As shown in Fig. 6d, only heparin caused a significant increase in relative RLS intensities of Ag NCs, while other species had no evident effect on the RLS intensities. The results demonstrated that physiological levels of cation, anion, amino acid and small biomolecules did not interfere with the detection. Specially, large

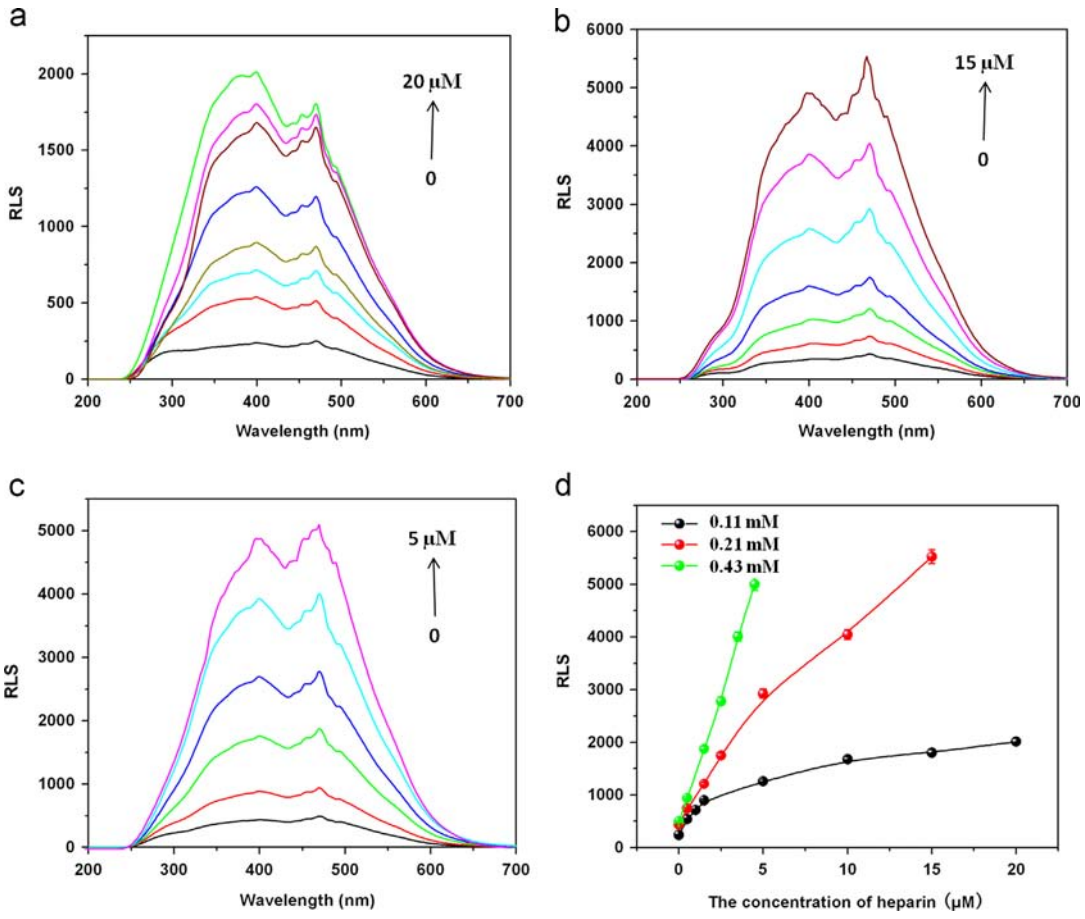

Fig. 7. Effect of PEI 1800-capped Ag NCs concentration on the RLS response to heparin: (a–c) RLS spectra (a, b and c refers to Ag NCs concentration at 0.11, 0.21 and 0.43 mM as Ag, respectively) and (d) plots of the RLS at 400 nm against the concentration of heparin.

Table 2
Analytical results for heparin in human serum samples.

Samples	Spiked (μmol L^{-1})	Measured (μmol L^{-1}) (mean ± S.D. $n=3$)	Recovery (%) (mean ± S.D. $n=3$)
1	0	N.D.	_
	1.0	1.1 ± 0.1	106.3 ± 5.3
2	0	N.D.	_
	3.0	2.8 ± 0.2	93.4 ± 6.4
3	0	N.D.	_
	5.0	4.9 ± 0.2	98.1 ± 4.4

molecules such as protein and calf thymus DNA at level of 5 μg mL^{-1} and 50 ng mL^{-1} did not interfere with the detection.

3.7. Application of the proposed method

The potential application of the proposed bioassay was further demonstrated by detecting heparin in human serum samples. The serum samples were ultrafiltrated to eliminate the RLS background of serum. The quantitative recoveries (93–106%) of spiked heparin also indicate no interference from such ultrafiltrated serum samples (Table 2). The above results demonstrate that the developed bioassay offers great potential for specific detection of heparin in biological fluids.

4. Conclusions

In summary, we have developed a facile green synthetic route for the preparation of highly fluorescent PEI-capped Ag NCs without extra addition of reducing agent. The proposed method demonstrates compellingly the potential utilization of the strategy by tuning the structure of template to green synthesis of other metal NCs. A RLS bioassay for heparin determination was established via a strategy of the target involved assembly of the prepared PEI-capped Ag NCs. This method exhibited a favorable linear range and satisfactory selectivity and successfully applied for heparin determination in human serum samples. The NCs will be used as excellent scaffolds for the foundation of resonance light scattering-based protocols to directly detect target molecules.

Acknowledgments

We appreciate the National Natural Science Foundation of China (Nos. 21075084 and 21105067), and State Key Laboratory of Electroanalytical Chemistry, Chinese Academy of Sciences (SKLEAC201102) for financial support. The authors also would like to show gratitude for Dr. Hong Chen of Analytical & Testing Center at Sichuan University for her assistance in the XPS analysis.

Appendix A. Supporting information

Supplementary data associated with this article can be found in the online version at http://dx.doi.org/10.1016/j.talanta.2013.06.028

References

[1] Y.Z. Lu, W. Chen, Chem. Soc. Rev. 41 (2012) 3594–3623.
[2] E. Gross, H.-C. LiuJack, F.D. Toste, G.A. Somorjai, Nat. Chem. 4 (2012) 947–952.
[3] X.X. Wang, Q. Wu, Z. Shan, Q.M. Huang, Biosen. Bioelectron. 26 (2011) 3614–3619.
[4] W. Chen, S.W. Chen, Angew. Chem. Int. Ed. 48 (2009) 4386–4389.
[5] O. Lopez-Acevedo, H. Tsunoyama, T. Tsukuda, H. Hakkinen, C.M. Aikens, J. Am. Chem. Soc. 132 (2010) 8210–8218.
[6] S.K. Sun, H.F. Wang, X.P. Yan, Chem. Commun. 47 (2011) 3817–3819.
[7] F. Qu, N.B. Li, H.Q. Luo, Anal. Chem. 84 (2012) 10373–10379.
[8] F. Qu, N.B. Li, H.Q. Luo, Langmuir 29 (2013) 1199–1205.
[9] X.L. Ren, Z.Z. Chen, X.W. Meng, D. Chen, F.Q. Tang, Chem. Commun. 48 (2012) 9504–9506.
[10] Y.C. Shiang, C.C. Huang, W.Y. Chen, P.C. Chen, H.T. Chang, J. Mater. Chem. 22 (2012) 12972–12982.
[11] Y.L. Xia, W.H. Li, M. Wang, Z. Ni, Z.Y. Deng, S.Z. Yao, Talanta 107 (2013) 55–60.
[12] L. Shang, S.J. Dong, G.U. Nienhaus, Nano Today 6 (2011) 401–418.
[13] P. Maity, S.H. Xie, M. Yamauchi, T. Tsukuda, Nanoscale 4 (2012) 4027–4037.
[14] H.W. Duan, S.M. Nie, J. Am. Chem. Soc. 129 (2007) 2412–2413.
[15] V. Sebastian, M. Pilar Calatayud, G.F. Goya, J. Santamaria, Chem. Commun. 49 (2013) 716–718.
[16] J.P. Xie, Y.G. Zheng, J.Y. Ying, J. Am. Chem. Soc. 131 (2009) 888–889.
[17] L. Shang, R.M. Dorlich, S. Brandholt, R. Schneider, V. Trouillet, M. Bruns, D. Gerthsen, G.U. Nienhaus, Nanoscale 3 (2011) 2009–2014.
[18] X. Yang, M.M. Shi, X.Q. Chen, H.Z. Chen, Nanoscale 3 (2011) 2596–2601.
[19] R.C. Jin, Nanoscale 2 (2010) 343–362.
[20] I. Diez, R.H.A. Ras, Nanoscale 3 (2011) 1963–1970.
[21] J.T. Petty, J. Zheng, N.V. Hud, R.M. Dickson, J. Am. Chem. Soc. 126 (2004) 5207–5212.
[22] Y.W. Zhou, C.M. Li, Y. Liu, C.Z. Huang, Analyst 138 (2013) 873–878.
[23] J.S. Mohanty, P.L. Xavier, K. Chaudhari, M.S. Bootharaju, N. Goswami, S.K. Pal, T. Pradeep, Nanoscale 4 (2012) 4255–4262.
[24] B. Adhikari, A. Banerjee, Chem. Eur. J. 16 (2010) 13698–13705.
[25] T.U.B. Rao, B. Nataraju, T. Pradeep, J. Am. Chem. Soc. 132 (2010) 16304–16307.
[26] X. Yuan, T.J. Yeow, Q.B. Zhang, J.Y. Lee, J.P. Xie, Nanoscale 4 (2012) 1968–1971.
[27] J. Zheng, R.M. Dickson, J. Am. Chem. Soc. 124 (2002) 13982–13983.
[28] Z. Shen, H. Duan, H. Frey, Adv. Mater. 19 (2007) 349–352.
[29] I. Diez, M.I. Kanyuk, A.P. Demchenko, A. Walther, H. Jiang, O. Ikkala, R.H.A. Ras, Nanoscale 4 (2012) 4434–4437.
[30] L. Shang, S.J. Dong, Chem. Commun. 44 (2008) 1088–1090.
[31] M. Manoth, K. Manzoor, M.K. Patra, P. Pandey, S.R. Vadera, N. Kumar, Mater. Res. Bull. 44 (2009) 714–717.
[32] T. Mikami, Y. Takayasu, J. Watanabe, I. Hirasawa, Chem. Eng. Technol. 34 (2011) 583–586.
[33] C. Aymonier, U. Schlotterbeck, L. Antonietti, P. Zacharias, R. Thomann, J.C. Tiller, S. Mecking, Chem. Commun. 38 (2002) 3018–3019.
[34] M. Baghbanzadeh, L. Carbone, P.D. Cozzoli, C.O. Kappe, Angew. Chem. Int. Ed. 50 (2011) 11312–11359.
[35] S.H. Liu, F. Lu, J.J. Zhu, Chem. Commun. 47 (2011) 2661–2663.
[36] J.R. Maurer, S. Haselbach, O. Klein, D. Baykut, V. Vogel, W. Mantele, J. Am. Chem. Soc. 133 (2010) 1134–1140.
[37] H. Yan, H.F. Wang, Anal. Chem. 83 (2011) 8589–8595.
[38] Y. Egawa, R. Hayashida, T. Seki, J.i. Anzai, Talanta 76 (2008) 736–741.
[39] R. Cao, B.X. Li, Chem. Commun. 47 (2011) 2865–2867.
[40] X.P. Sun, S.J. Dong, E.K. Wang, Mater. Chem. Phys. 96 (2006) 29–33.
[41] H.S. Shin, H.J. Yang, S.B. Kim, M.S. Lee, J. Colloid Interface Sci. 274 (2004) 89–94.
[42] S.L. Tan, M. Erol, A. Attygalle, H. Du, S. Sukhishvili, Langmuir 23 (2007) 9836–9843.
[43] X.P. Sun, Y.L. Luo, Mater. Lett. 59 (2005) 3847–3850.
[44] T.A.C. Kennedy, J.L. MacLean, J. Liu, Chem. Commun. 48 (2012) 6845–6847.
[45] Z.L. Jiang, L.P. Zhou, A.H. Liang, Chem. Commun. 47 (2011) 3162–3164.
[46] W.J. Qi, D. Wu, J. Ling, C.Z. Huang, Chem. Commun. 46 (2010) 4893–4895.
[47] Z.L. Jiang, S.M. Wang, A.H. Liang, F.X. Zhong, Talanta 77 (2009) 1191–1196.
[48] C. Xiong, L.S. Ling, Talanta 89 (2012) 317–321.